Purification and Initiation of Structural Characterization of Human Peripheral Myelin Protein 22, an Integral Membrane Protein Linked to Peripheral Neuropathies†

Charles K. Mobley, Jeffrey K. Myers, Arina Hadziselimovic, Charles D. Ellis, and Charles R. Sanders*

Department of Biochemistry and Center for Structural Biology, Vanderbilt University School of Medicine, Nashville, Tennessee 37232-8725

Received May 5, 2007; Revised Manuscript Received July 28, 2007

ABSTRACT: Gene duplications, deletions, and point mutations in peripheral myelin protein 22 (PMP22) are linked to several inherited peripheral neuropathies. However, the structural and biochemical properties of this very hydrophobic putative tetraspan integral membrane protein have received little attention, in part because of difficulties in obtaining milligram quantities of wild type and disease-linked mutant forms of the protein. In this study a fusion protein was constructed consisting of a fragment of lambda repressor, a decahistidine tag, an intervening TEV protease cleavage site, a Strep tag, and the human PMP22 sequence. This fusion protein was expressed in *Escherichia coli* at a level of 10−20 mg/L of protein. Following TEV cleavage of the fusion partner, PMP22 was purified and its structural properties were examined in several different types of detergent micelles using cross-linking, near and far-UV circular dichroism, and nuclear magnetic resonance (NMR) spectroscopy. PMP22 is highly helical and, in certain detergents, shows evidence of stable tertiary structure. The protein exhibits a strong tendency to dimerize. The $^{1}H-^{15}N$ TROSY NMR spectrum is well dispersed and contains signals from all regions of the protein. It appears that detergent-solubilized PMP22 is amenable to detailed structural characterization via crystallography or NMR. This work sets the stage for more detailed studies of the structure, folding, and misfolding of wild type and disease-linked mutants in order to unravel the molecular defects underlying peripheral neuropathies.

Peripheral myelin protein 22 (PMP22,[1] also known as growth arrest specific protein 3; NCBI NP_000295) is a hydrophobic 160 amino acid membrane protein that has cytosolic N- and C-termini (*1*−*3*) (Figure 1). PMP22 is a member of a family of homologous membrane proteins, termed the PMP22/EMP/MP20/Claudin superfamily (pfam00822 in NCBI), which are recognizable by sequence homology along with their predicted tetraspan topology (*4*, *5*). That PMP22 actually has four transmembrane segments, however, remains unconfirmed. In fact, an epitope tagging/accessibility study led to a proposal that PMP22 has only 2 transmembrane segments (*6*). PMP22 is highly expressed in the Schwann cells of the peripheral nervous system (PNS), where it makes up 2−5% of the total membrane protein in compact myelin (*6*, *7*). PMP22 is also expressed at lower levels in a variety of tissues (*8*, *9*). The higher level in the PNS is related to the presence of two different promoters, one of which appears to specifically drive PMP22 gene expression (*9*).

The functions of PMP22 are still being elucidated. In the PNS, PMP22 is involved in promoting and maintaining the myelin sheath (*10*−*14*). Myelin can be regarded as a specialized domain of the plasma membrane of Schwann and oligodendrocyte cells that wraps around adjacent axons to serve as electrical insulation to promote rapid propagation of the action potential between axonal nodes of Ranvier (*15*, *16*). Adhesion between the layers of myelin membrane is thought to be mediated primarily by myelin protein zero (MPZ) (*17*). PMP22 has been shown to interact with MPZ and may assist MPZ in its adhesive function (*18*−*20*). Additional proposed functions of PMP22 include regulation of the cell cycle and cellular proliferation (*7*, *21*−*24*), a role in formation of cell−cell or myelin-specific junctions (*18*, *25*, *26*), and mediation of interactions between the basal lamina and Schwann cells (*27*). Other hints for PMP22's functions are suggested by homology to the claudins and the TARPs (*4*, *5*, *28*−*31*). PMP22 also shares a distinctive sequence motif (*4*) in its extracellular domain with the connexins, tetraspan membrane proteins that form hemichannels that span juxtaposed membranes in epithelia (*4*, *32*−*34*).

† This study was supported by grants from the Muscular Dystrophy Association (MDA3702 to J.K.M. and a pilot grant to C.R.S.) and by the US NIH (R21 N5048573 and R01 GM47485 to C.R.S.).

* To whom correspondence should be addressed. E-mail: chuck.sanders@vanderbilt.edu. Phone: 615-936-3756. Fax: 615-936-2211.

[1] Abbreviations: CMTD, Charcot−Marie−Tooth disease; CD, circular dichroism; DDM, *n*-dodecyl-*β*-D-maltopyranoside; DM, *n*-decyl-*β*-D-maltopyranoside; DPC, dodecylphosphocholine; DSS, Dejerine−Sottas syndrome; Empigen, trade name for *n*-dodecyl-*N*,*N*-dimethylglycine; ER, endoplasmic reticulum; HNPP, hereditary neuropathy with liability to pressure palsies; LDAO, *N*-lauryldimethylamine oxide; LMPC, 1-myristoyl-2-hydroxy-*sn*-glycero-3-phosphocholine; LMPG, 1-myristoyl-2-hydroxy-*sn*-glycero-3-[phospho-1-(l-glycerol)]; LS, lauroylsarcosine; MPZ, myelin protein zero; MtBP, maltose binding protein; MS, mass spectrometry; NCBI, National Center for Biotechnology Information; NMR, nuclear magnetic resonance; PMP22, peripheral myelin protein 22; PNS, peripheral nervous system; SDS, sodium dodecyl sulfate; TDPC, tetradecylphosphocholine; TEV, tobacco etch virus.

10.1021/bi700855j CCC: $37.00
Published on Web 09/07/2007

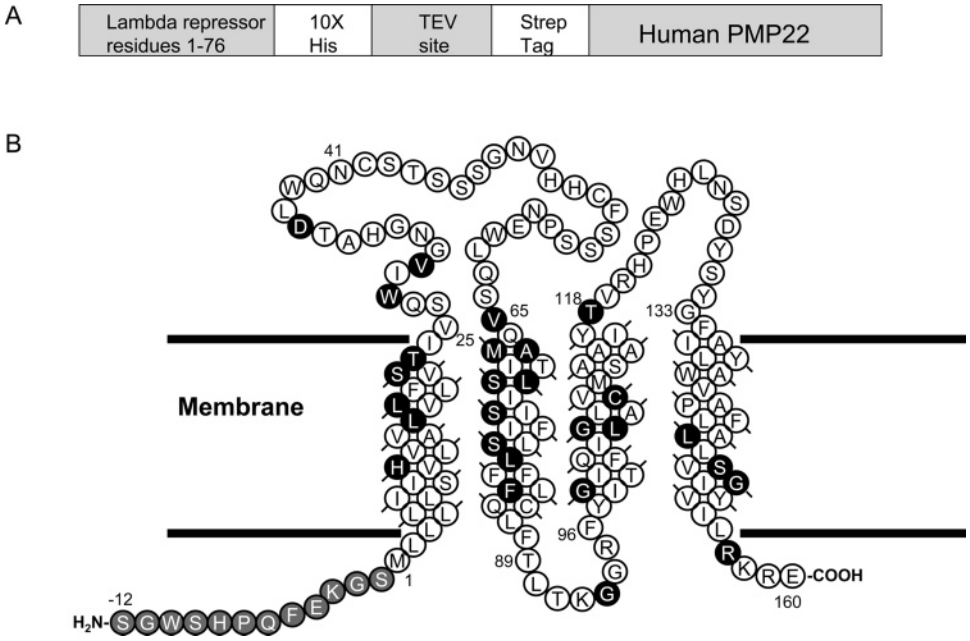

FIGURE 1: Expression construct and sequence of PMP22. (A) Diagram of the fusion protein targeted for heterologous expression in *E. coli*. (B) Amino acid sequence of the final purified form of PMP22 studied in this work, showing the predicted locations of transmembrane segments. Sites of disease-linked missense mutations (*101*) are shown in black, and residues added to the N terminus are indicated in gray. It should be noted that while predicted to have 4 transmembrane segments and homologous to a number of other proteins for which the same prediction is made, there is experimental evidence that the loop connecting the depicted second and third transmembrane segments is actually extracellularly located, suggesting that PMP22 only has two transmembrane segments (the N- and C-termini) (*6*).

The importance of PMP22 is highlighted by its association with several diseases of the PNS, including Charcot−Marie−Tooth disease, the most common hereditary peripheral neuropathy (*7*, *35*−*37*). Disease can result from changes in gene dosage or mutations in the PMP22 gene, for which the severity of the phenotype is dependent on the exact nature of the mutation. Dominant mutations typically lead to single amino acid changes in PMP22 that result in misassembly of the protein, resulting both in loss of PMP22 function and, it is believed, in the toxic accumulation of misfolded PMP22 in the cell (*38*−*46*). The most common form of Charcot−Marie−Tooth disease is caused by the presence of a third wild type allele (*47*), while rare homozygous duplication of both alleles results in a very severe form of neuropathy, DSS, symptoms of which can be modeled in rats and mice by transgenic overexpression of PMP22 (*48*, *49*). In these cases, dysfunction may be triggered by too-high levels of wild type PMP22 combined with possible toxicity resulting from accumulation of the fraction of the protein that misassembles and then is not properly degraded (*24*, *50*). It should be pointed out that, even under normal homozygous conditions, wild type PMP22 folds very inefficiently, with only ∼20% of the protein produced reaching the myelin membrane (*4*, *51*).

In order to understand the subtle and complex effects of the disease-linked mutations, it is necessary to elucidate their effects on the structure, folding, and stability of PMP22, issues that require molecular biophysical characterization. For such studies, it is necessary to obtain milligram quantities of purified protein. While protocols have been published to obtain PMP22 from bovine nerves (*52*−*54*), these methods require working with PNS tissue. This approach also does not yield the actual disease-relevant *human* isoform. Finally, there is no convenient route to obtaining disease-linked mutant forms from animal tissues or to isotopically label the protein for use in NMR studies. An attractive alternative route would be to establish a heterologous expression system for PMP22 to generate large amounts of both wild type and mutant protein in labeled and unlabeled forms. Here, we report that by expressing PMP22 with a fusion partner in *Escherichia coli*, proteolytically removing the fusion partner, and then purifying the protein, it is possible to reproducibly generate 5−10 mg of pure PMP22 per liter of culture. Also reported are the results of biophysical characterization, which indicates that PMP22 is a folded helical dimer in mild detergent solutions. Moreover, preliminary NMR data suggests that determination of a high-resolution three-dimensional structure is feasible.

MATERIALS AND METHODS

Production of His_6-TEV Protease for Use in Cleavage of the PMP22 Fusion Protein. A fusion protein composed of maltose binding protein (MtBP) followed by a His_6 tag, followed by tobacco etch virus protease (TEV), was encoded and expressed from a pS219V vector in Rosetta (DE3) *E. coli* cells (*55*). An initial overnight culture of 12 mL of LB medium containing 100 μg/mL ampicillin and 50 μg/mL chloramphenicol was grown from a single cell colony for a minimum of 12 h. This culture was then added to a liter of LB containing the antibiotics in the same concentrations. The cells were grown at 37 °C in a shaking incubator until they reached an OD_{600} of 0.6, at which point the temperature was reduced to 15 °C and the cells were induced by adding isopropyl-β-D-1-thiogalactopyranoside (IPTG) to a final concentration of 1 mM. Upon expression, MtBP is autocleaved from the fusion protein *in situ* by TEV protease. The cells were harvested 12 h after induction, and 20 mL of lysis buffer (50 mM dibasic sodium phosphate, 100 mM NaCl, 10% glycerol, pH 7.4) at 4 °C was added for each gram of wet cells. Phenylmethanesulfonyl fluoride (PMSF)

was added to a concentration of 1.1 mM, and dithiothreitol (DTT) was added to 0.5 mM. The cells were tumbled or shaken at 4 °C until fully dispersed, and then lysed by two passes through an EmulsiFlex C3 homogenizer.

In all subsequent steps solutions were maintained at 4 °C to keep TEV protease from precipitating. The lysate was centrifuged at 12900*g* for 30 min, after which the supernatant was poured through cheesecloth and tumbled with lysis-buffer-equilibrated Qiagen Superflow Ni-NTA resin (1.2 mL of resin per gram of original cell pellet). After 45 min, the resin was poured into a chromatography column and then washed with 10 bed volumes of ice cold wash buffer 1 (50 mM dibasic sodium phosphate, 100 mM NaCl, 10% glycerol, 0.5 mM DTT, pH 7.4). The resin was next washed with 10 bed volumes of ice cold wash buffer 2 (50 mM sodium phosphate, 100 mM NaCl, 10% glycerol, 25 mM imidazole, 0.5 mM DTT, pH 7.4). The protein was eluted from the column using elution buffer (100 mM NaCl, 20% glycerol, 250 mM imidazole, 0.5 mM DTT, pH 7.5). The DTT concentration of the eluted protein solution was then increased to 10 mM (to prevent oxidation of the free thiol in the TEV protease active site), and the solution was dialyzed for at least 12 h in 50 mL aliquots against 2 L of 20 mM dibasic sodium phosphate, 300 mM NaCl, 20% glycerol, 10 mM DTT, pH 7.0. The dialysis tubing used was SpectraPor-1 with a molecular weight cutoff of 6−8 kDa.

Because the Ni-NTA column is only partly successful at removing cleaved maltose binding protein, a second column was run. For every 20 mL of dialyzed TEV solution, 5 mL of amylose resin (New England Biolabs, Ipswich, MA; equilibrated with 50 mM sodium phosphate buffer at pH 7.0) was added to the solution. This was then tumbled for 1 h in order to remove any residual contaminating MtBP generated by autocleavage of the fusion protein. After removal of the amylose resin, the protein concentration was determined by absorbance at 280 nm using an estimated extinction coefficient of 37400 M^{-1} cm^{-1} (1.31 mL mg^{-1} cm^{-1}). 60 mL glycerol and 15 mL of storage mix (50% glycerol, 10 mM DTT, 90 mM Tris-HCl, 2 mM EDTA, 0.2% Triton X-100, 160 mM NaCl, pH 7.5) were then added per 100 mL of TEV solution. The solution was mixed, frozen in liquid nitrogen, and stored at −80 °C until used to cleave the PMP22 fusion protein. The final solution usually had a TEV concentration of ∼0.8 mg/mL.

Overexpression of PMP22. The PMP22 gene (GenBank nucleotide database entry NM_153321) was a kind gift of Drs. P. Berger and U. Suter (Department of Biology, ETH, Zurich). The gene was cloned into the pAH1.96 expression plasmid (*63*) (courtesy of R. Breyer, Vanderbilt University) using PCR and unique *Bam*HI and *Hin*dIII restriction sites. The thrombin site of the original plasmid was replaced with a TEV recognition site, the 6x His tag was replaced by a 10x His, and a Strep tag (*56*) was added to act as a spacer between the TEV site and PMP22. This new plasmid was sequenced to confirm the integrity of its sequence and is designated pAH11/strPMP22. This construct confers ampicillin resistance and features an IPTG inducible promoter for the fusion protein, which combines the first 76 residues of lambda repressor and human PMP22 (see Figure 1A). The fusion protein is expressed in RosettaBlue *E. coli* cells (Novagen) that contain an additional plasmid encoding rare codon tRNAs. Freezer stocks of the expression plasmid in RosettaBlue cells in LB/glycerol appear to be stable.

The expression of the lambda-PMP22 fusion protein was initiated by inoculating 10 mL of LB medium containing 100 μg/mL ampicillin and 50 μg/mL chloramphenicol at 37 °C for at least 12 h. This was added to a liter of sterile minimal medium (40 mM Na_2HPO_4, 20 mM KH_2PO_4, 10 mM NaCl, 20 mM NH_4Cl, 0.1 mM $CaCl_2$, 1 mM $MgSO_4$, 0.4% glucose, at pH 7.0) containing antibiotics at the same concentrations. Minimal medium also included 5 mL of vitamin solution made by crushing a CVS Spectravite multivitamin/multimineral tablet and dissolving in 40 mL of distilled water, discarding insoluble material. The cultures were grown at 20 °C for 24 h (or an $OD_{600} = 0.100$) at which point an additional 1 mL of 100 mM ampicillin was added to replace that lost through action of β-lactamase (a typical OD_{600} value after 24 h is 0.14). Growth was continued until the culture reached an $OD_{600} = 1$ (an additional 24 to 48 h), at which point IPTG was added to 1 mM. Induction was continued for a minimum of 16 h before the cells were harvested by centrifugation at 12900*g*. The cell pellet was stored until purification at −80 °C in lysis buffer (75 mM Tris-HCl, 300 mM NaCl, 0.2 mM EDTA, 10 μM BHT, pH 7.5) containing 4 mg/mL PMSF.

Purification of the PMP22 Fusion Protein. Additional lysis buffer was added to cells prepared as described above to raise the total volume to 20 mL per gram of cell pellet. Lysozyme (0.2 mg/mL of total lysis buffer volume), RNase (0.02 mg/mL), and DNase (0.02 mg/mL) were added, and the solution was incubated at 4 °C for 30 min with agitation. Magnesium acetate was added to a concentration of 5 mM, and the lysate was then sonicated on ice for 10 min using a Fisher Scientific 550 Sonic Dismembrator. DTT was then added to a concentration of 0.5 mM.

To extract the fusion protein from the plasma membrane of the lysed cells, the solution was made 15% in glycerol and 3% in Empigen (a harsh detergent, Calbiochem, La Jolla, CA) and the solution was tumbled at 4 °C for 45 min. After centrifugation at 15000*g* and 4 °C for 20 min, the supernatant was poured through cheesecloth into a clean bottle. Ni-NTA resin (1.2 mL of resin per gram of cell pellet) was equilibrated with 4 column volumes of buffer A (40 mM HEPES, 300 mM NaCl at pH 7.5) and added to the clarified lysate. This mixture was tumbled for 45 min at 4 °C, and the resin was then packed into a chromatography column. The fusion protein was then purified from this column through the addition of four buffers, starting with 5 bed volumes of ice cold Emp/A buffer (40 mM HEPES, 300 mM NaCl, 15% glycerol, 3% Empigen, 0.5 mM DTT at pH 7.5). This was followed by ice cold wash buffer (40 mM HEPES, 30 mM imidazole, 300 mM NaCl, 15% glycerol, 1.5% Empigen, 0.5 mM DTT at pH 7.8) until the measured A_{280} indicated complete elution of weakly bound impurities, usually ∼4 bed volumes. The protein was then exchanged from an Empigen solution into a solution containing *N*-dodecylphosphocholine (DPC, from Anatrace) as the detergent component by passing 10 × 1 bed volumes of ice cold rinse buffer through the column (0.5% DPC, 25 mM sodium phosphate, 0.5 mM DTT at pH 7.2). Finally, the protein was eluted from the column using ice cold elution buffer (0.5% DPC, 250 mM imidazole, 50 mM Trizma-HCl, and 0.5 mM DTT at pH 8.0). Measurement of A_{280} was used to determine the protein concentration using an estimated extinction coefficient of 49700 M^{-1} cm^{-1} (1.64 mL mg^{-1} cm^{-1}) before

diluting with elution buffer to a concentration of 0.8 mg/mL in preparation for TEV cleavage.

Removal of the Fusion Partner and Purification of PMP22. The fusion protein was cleaved by mixing an equal volume of TEV protease and eluted fusion protein solutions (both at 0.8 mg/mL) and incubating at room temperature for 24−48 h. The buffer contained 25% glycerol, 0.25% DPC, 0.0075% Triton X-100, 130 mM imidazole, 30 mM Tris, 6 mM sodium phosphate, 0.1 mM EDTA, 90 mM NaCl, 3 mM DTT, pH 7.5. The cleavage reaction was then incubated at 30 °C for an additional 24 h, during which time TEV gradually precipitated from solution. The TEV precipitate was removed by centrifugation at 25000*g* for 20 min at 4 °C.

In order to remove several contaminants (including the lambda repressor portion of the fusion protein) and, if desired, to exchange PMP22 from DPC into another detergent, we performed ion exchange chromatography. The pH of the cleavage reaction solution was reduced to 5.0 with acetic acid and then filtered through a 0.45 μm HA membrane. The solution was then purified on an 8 mL Mono S cation exchange column using an Akta Purifier FPLC system. Typically 35−45 mL of 0.4 mg/mL PMP22 was loaded on the column. All purification solutions were filtered before use. The buffer used was 50 mM acetate, 0.5 mM DTT, pH 5.0 with 0.2% of detergent. Detergents used included DPC, 1-myristoyl-2-hydroxy-*sn*-glycero-3-phosphocholine (LMPC), *N*-tetradecylphosphocholine (TDPC), *n*-decyl-β-D-maltopyranoside (DM), and *n*-dodecyl-β-D-maltopyranoside (DDM) (LMPC from Avanti Polar Lipids, all other detergents from Anatrace). Protein was eluted using an 80 mL, 0 to 0.65 M NaCl gradient in the same buffer at a flow rate of 1.5 mL/min, collecting the eluate in 2 mL fractions. Fractions containing PMP22 were identified using SDS−PAGE. To the combined fractions we added 1 mL of Ni-NTA (preequilibrated in pH 5.0 acetate buffer) for every 30 mL of PMP22 and tumbled at 4 °C for 45 min to remove any remaining fusion protein and TEV protease. After removal of the resin, DTT was added to 10 mM and the solution was concentrated in a 5,000 Da MWCO Amicon Ultra-15 centrifugal filtering device (Millipore). The resulting stock solution was then stored at 4 °C until use. Stock solution concentrations were obtained by UV absorbance using an estimated extinction coefficient at 280 nm of 44880 M^{-1} cm^{-1} (2.33 mL mg^{-1} cm^{-1}).

Confirmation of Strep-Tagged PMP22 by Mass Spectrometry. The identity of purified Strep-tagged PMP22 was confirmed both by intact mass determination and by peptide mass and fragmentation patterns using mass spectrometry. For intact mass determination the protein was dialyzed against a solution that consisted of water:isopropanol:formic acid (3:2:1) for 7 days, replacing the dialysis buffer with fresh buffer every 2 days. After dialysis the protein had a concentration of 1.2 mg/mL. The dialyzed protein (1 μL) was mixed with 2 μL of ferulic acid solution (40 mg of ferulic acid in 1 mL of 60% acetronitrile, 40% water, and 0.1% trifluoroacetic acid), and 1 μL was then spotted onto a gold sample target for matrix-assisted laser desorption/ionization time-of-flight mass spectrometry (MALDI-TOF MS) using a Voyager DE-STR (Applied Biosystems) operated in the linear positive ion mode with delayed extraction. The acquired mass spectrum was processed using a standard noise filter (0.7) and smoothing algorithm (7 pt), yielding an intact molecular mass (M + H) of *m*/*z* 19283.9. The 0.33% difference between this and the expected *m*/*z* of 19220.6 is within the error of measurement for this protein (peak width at half-maximal height = 907).

For further confirmation, a band corresponding to full-length PMP22 was excised from an SDS−PAGE gel after staining with coomassie blue and subjected to in-gel digestion with either trypsin or chymotrypsin protease using standard procedures (*57*). Extracted peptides were analyzed by MALDI-TOF MS as well as by tandem TOF/TOF MS to produce peptide fragmentation data using a Voyager 4700 (Applied Biosystems). Tandem MS data were also acquired by ESI-LC/MS/MS using an LTQ linear ion trap mass spectrometer (ThermoFisher) using standard operating procedures (*58*). These methods confirmed the presence of the predicted N-terminal peptide SGWSHPQFEK, as well as several other peptides predicted from the protein sequence (IVGNGHATDLW, QNCSTSSSGNVHHCF, TVRHPEW, and HLNSDYSYGFAY), collectively spanning over 85% of the predicted protein sequence.

Cross-Linking of PMP22. Cross-linking reactions were performed at room temperature using 0.75% formaldehyde for 16 h. PMP22 was incubated in pH 5.5 acetate buffer with 1.5% of the particular detergent tested in the presence of 10 mM DTT for several hours before formaldehyde was added.

Circular Dichroism. Circular dichroism (CD) experiments were performed using a Jasco J-810 instrument with a Peltier temperature controller and a magnetic stirrer. Samples were placed in either 1 cm or 0.1 cm path length quartz cuvettes. Spectra were acquired at 20 °C, with a 1.5 nm bandwidth and 4 s of averaging at each wavelength. Three spectra were averaged to give the final trace. Protein concentrations were 10 μM (ca. 0.2 mg/mL) in a 0.1 cm cell for far-UV CD or 26 μM in a 1 cm cell for near-UV CD.

NMR Samples and Spectroscopy. Uniformly-^{15}N-labeled PMP22 for NMR studies was produced as described above, with the exception that ^{15}N-labeled ammonium chloride (Cambridge Isotopes Lab, Andover, MA) was used in the minimal media. A modified procedure was employed to generate uniformly-^{2}H,^{13}C,^{15}N-labeled PMP22. 5 mL of overnight LB culture of RosettaBlue harboring pAH11/strPMP22 was added to 50 mL of unlabeled minimal medium. This was allowed to grow at 37 °C to an OD_{600} = 0.5, at which time 0.5 mL was added to 50 mL of minimal medium containing 70% deuterium oxide. This was grown at 37 °C until it reached an OD_{600} = 0.5, at which point a 0.5 mL aliquot was taken and added to 50 mL of minimal medium containing 99% deuterium oxide, ^{15}N ammonium chloride, and $^{13}C_6$-glucose. This culture was grown at 37 °C until OD_{600} = 0.5, at which point this culture was used to inoculate 4 × 1 L of the same triple-labeled minimal medium (10 mL of the small culture for each 1 L flask). These cultures were then grown at 20 °C and harvested under the conditions described above for unlabeled PMP22.

Following purification as described in the previous section NMR samples were prepared by concentrating purified labeled PMP22 to 5 mL and then adding 0.54 mL of D_2O and 0.05 mL of 100 mM EDTA, pH 7.0. The solution was then further concentrated to 600 μL and placed in a 5 mm NMR tube. Spectra were acquired at 45 °C and pH 5.0 on

a Bruker 800 MHz spectrometer equipped with a 5 mm CPTCI-Z cryo-probe.

^{1}H,^{15}N-Correlation NMR spectra were acquired using the Weigelt TROSY pulse sequence with ^{13}C-decoupling (*59*). A constant time TROSY-HNCA was carried out using an in-house-coded sequence (*60*). Spectra were processed using NMRPipe (*61*).

RESULTS

Expression and Purification of PMP22. A formidable barrier to the structural characterization of vertebrate membrane proteins is the imperative to purify milligram quantities of protein. While PMP22 has previously been expressed in *E. coli* to a level sufficient for immunological detection (*62*), extensive efforts to overexpress PMP22 in the absence of a fusion partner in *E. coli* via the pET21b or other expression vectors resulted in only low expression levels. More favorable results were obtained using a fusion protein in which the first 76 residues of the water-soluble lambda repressor were fused to PMP22's N-terminus via a cleavable linker (Figure 1A). The utility of lambda repressor fusions for overexpressing multispan eukaryotic membrane proteins was previously demonstrated by the lab of R. Breyer (*63*), although the reasons for its efficacy are not well understood. We tested the expression of the fusion protein in two cell types: RosettaBlue and C43(DE3) strains of *E. coli*. For each, expression was tested in rich vs minimal media and at 20 °C vs 37 °C. Strong expression was observed in RosettaBlue but not in C43(DE3). Expression was much higher in minimal media than in rich media, and was also higher for 20 °C cultures as opposed to 37 °C. Lowering the temperature to 12 °C did not further enhance expression. Under optimal growth conditions and following subcellular fractionation, the fusion protein was found to be expressed primarily into the *E. coli* plasma membrane. Random cross-linking of the expressed protein in *E. coli* using formaldehyde or glutaraldehyde followed by SDS−PAGE and Western blot detection shows that most of the recombinant fusion protein forms high molecular weight aggregates (not shown). Expression of a human membrane protein into the membrane of *E. coli* (as opposed to expression into inclusion bodies) is not a guarantee that the protein will be folded properly.

After purification of the fusion protein using metal ion affinity chromatography, PMP22 was released from its lambda repressor partner using TEV protease. PMP22 was isolated from both its cleaved fusion partner and the TEV protease via cation exchange chromatography. An SDS−PAGE gel documenting the various stages of purification is shown in Figure 2. Mass spectrometry confirmed the identity of the final Strep-tagged PMP22. It should be noted that both the intact fusion protein (lane 5) and the purified PMP22 (lanes 9 and 10) run at apparent molecular weights that are several kDa lower than expected (ca. 30, and 18 kDa, respectively). This reflects the commonly observed phenomenon that multispan helical membrane proteins often run anomalously fast on SDS−PAGE gels. This procedure results in 5−10 mg of pure PMP22 per liter of starting culture. The amino acid sequence of the recombinant PMP22, the predicted regions of the transmembrane segments, and the locations of disease-linked point mutations are shown in Figure 1B.

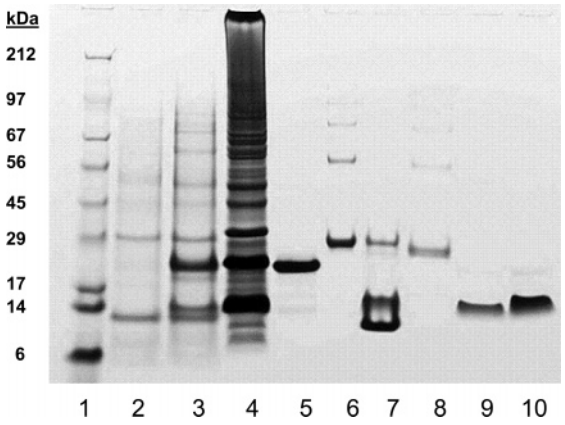

FIGURE 2: Coomassie-stained SDS−PAGE of samples from a typical PMP22 purification run. Lane 1, molecular weight markers; lane 2, preinduction whole cell; lane 3, post-induction whole cell; lane 4, whole cell lysate; lane 5, purified fusion protein; lane 6, TEV protease used for cleavage; lane 7, fusion protein cleavage reaction; lane 8, TEV pellet from cleavage reaction; lane 9, PMP22 after ion exchange chromatography; lane 10, final concentrated PMP22 solution.

Examination of the Oligomeric State of PMP22. In vivo, PMP22 has been shown to form dimers and possibly higher order oligomers (*64*−*66*). In order to probe the quaternary structure of purified PMP22 we used chemical cross-linking with formaldehyde (Figure 3A). The protein exhibits a strong tendency to form dimers in nondenaturing detergents, including DPC, DM, TDPC, and (to a lesser extent) LMPC. All of these detergents also sustained formation of tertiary structure, as shown by near-UV CD (see below). On the other hand, PMP22 remains monomeric after cross-linking in harsh detergents such as SDS. Cross-linking results similar to those depicted in Figure 3A were also obtained using glutaraldehyde as the cross-linking agent, but the efficiency of cross-linking was sometimes lower than observed when formaldehyde was used. In the absence of a thiol reducing agent, PMP22 also exhibits a strong tendency to form disulfide-bonded dimers upon prolonged incubation under a normal atmosphere (Figure 3B).

Near- and Far-UV Circular Dichroism of PMP22. In order to probe the secondary and tertiary structure of PMP22 we employed near- and far-UV circular dichroism spectroscopy (CD). The far-UV CD spectrum of PMP22 in DPC micelles is consistent with a largely helical secondary structure (Figure 4A). Analysis using the K2D program (*67*) indicates roughly 65% helix, 5% beta, and 30% random coil. The predicted transmembrane helical regions make up about 50% of the sequence, and it is easy to imagine the remaining 15% of helical content to reside in the extramembrane segments. Helicity was observed to be retained even in SDS, which is not surprising given the general ability of SDS micelles to support helix formation in many amino acid sequences (*68*).

Near-UV (250−310 nm) circular dichroism arises from the spatial ordering of tryptophan, tyrosine, and phenylalanine side chains, as well as disulfide bonds (if present), and is therefore sensitive to protein tertiary structure (*69*−*74*). Unfolded or molten globular proteins, for which the aromatic side chains are disordered, do not yield a CD spectrum in this region. The significant negative signal shown in Figure 4B is consistent with a well-ordered tertiary structure. Of the ca. 20 membrane proteins for which we have acquired

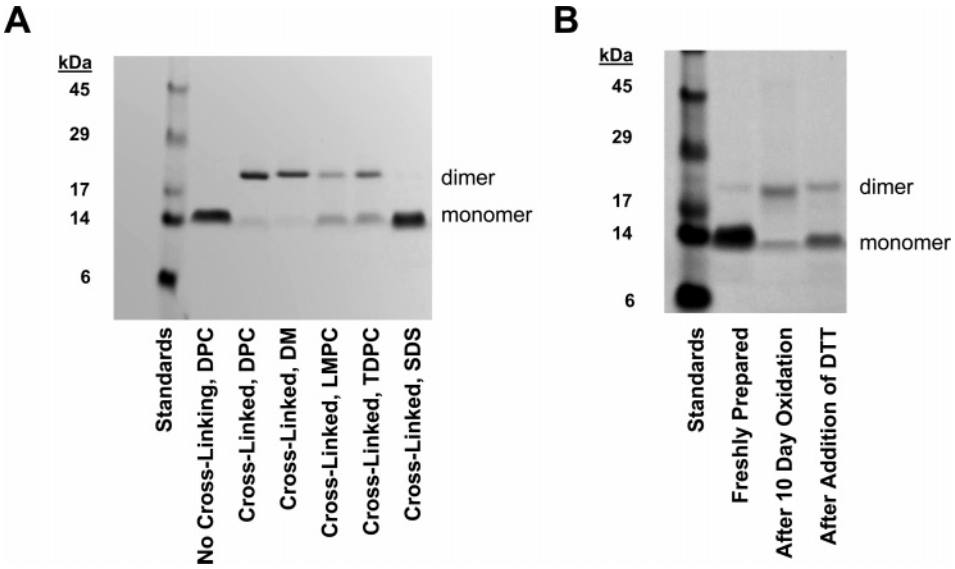

FIGURE 3: PMP22 has a tendency to dimerize and also to form disulfide bonds. (A) SDS−PAGE/coomassie of PMP22 in various detergents following cross-linking by formaldehyde. Samples also contained 10 mM dithiothreitol (DTT) to prevent disulfide bond formation. (B) SDS−PAGE/coomassie of PMP22 in DPC micelles immediately after preparation, after room temperature exposure to the atmosphere for 10 days in the absence of a reducing agent, and after DTT reduction (20 mM, overnight) of the protein following the 10-day oxidation.

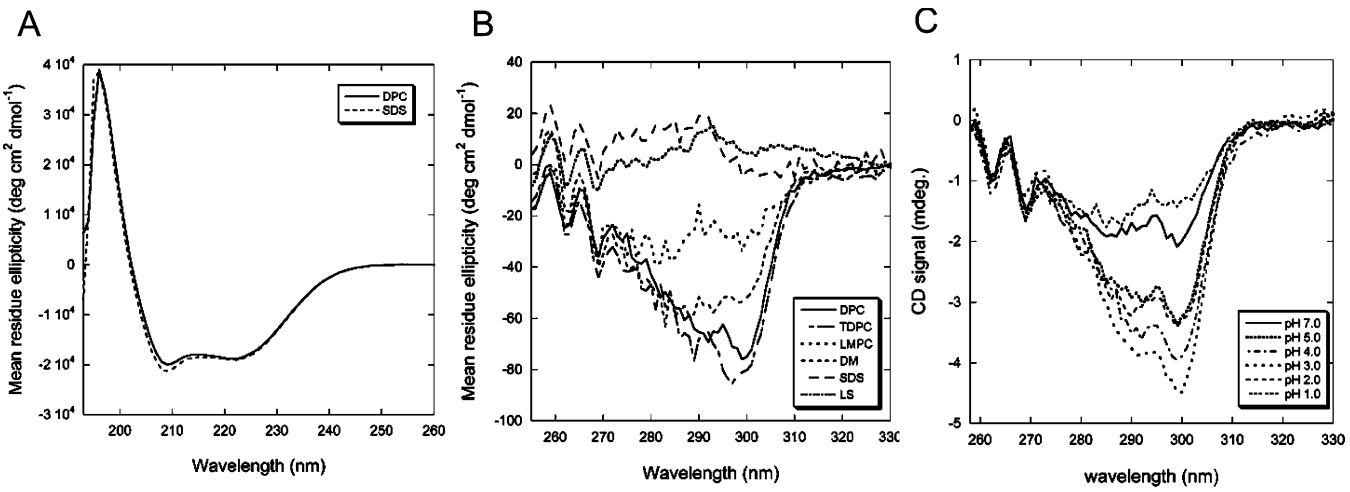

FIGURE 4: Circular dichroism (CD) spectroscopic analysis of PMP22 at 20 °C. (A) Far-UV CD spectra of PMP22 in 0.5% DPC and 1.5% SDS detergent micelles showing the characteristic double minima at 208 and 222 nm, indicative of significant α-helical content. The protein concentration was 10 μM, and the buffer contained 25 mM acetate, pH 5.5. (B) Near-UV CD spectra of PMP22 in various detergents, showing differences in tertiary structure. The protein concentration was 26 μM, and the buffer was the same as for A. The various detergents were present at 0.5%. (C) Near-UV CD spectra of PMP22 in DPC micelles as a function of pH.

near-UV CD data (unpublished), PMP22 exhibits one of most intense spectra. The intensity and shape of PMP22's spectrum depends on the detergent used to solubilize the protein, with the closely related alkylphosphocholines TDPC and DPC giving the most intense spectra. The tertiary structure appears to be completely disrupted in harsh detergents such as SDS or lauroylsarcosine. The structure also appears to be pH-sensitive, with the maximum signal being observed at pH 3, and falling away at either extreme (Figure 4C). At pH 7 there is about half the signal observed at pH 3, while at pH 1 the protein appears to be mostly unfolded. The changes in the spectrum are most pronounced near 300 nm, where Trp side chains (PMP22 has 6) are expected to dominate the spectrum, whereas there is little pH-dependent change in the 260−270 nm regime, which is expected to be dominated by Phe side chains (PMP22 has 12). Given that 4 out of 6 Trp residues in PMP22 are located outside of the membrane, with one of the remaining Trp being located in the N-terminal Strep tag (which is expected to be disordered such that its single Trp is not expected to contribute to the near-UV CD signal), this suggests that the extracellular domain undergoes pH-dependent changes in conformation. On the other hand, the fact that 11 of the 12 Phe residues in PMP22 proper are located within the transmembrane domain (assuming the tetraspan model is correct) suggests that the structure of this domain is relatively pH independent.

NMR Spectrum of PMP22. PMP22 was produced in minimal medium containing ^{15}N-labeled ammonium chloride as the sole nitrogen source. Extensive screening was carried out to determine the best conditions for NMR. A variety of detergents were tested, including DPC, TDPC, LMPC, DM, DDM, and LDAO. Negatively charged detergents were not screened because they either unfold the protein (e.g., SDS) or interfered with the binding of PMP22 to the MonoS column during the final step of purification (in the case of LMPG). The protein appeared to be stable in all of the

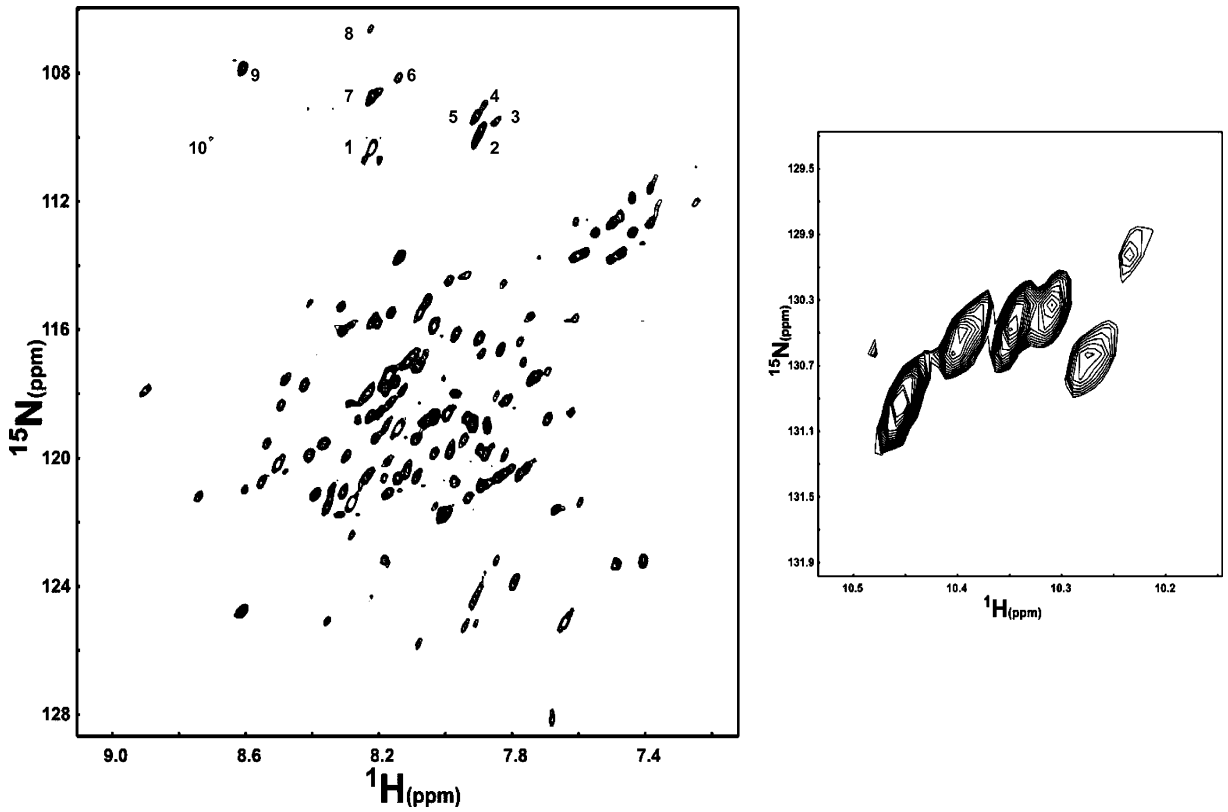

FIGURE 5: NMR spectrum of uniformly ^{2}H,^{13}C,^{15}N-labeled PMP22. (A) Two-dimensional 800 MHz ^{1}H−^{15}N-TROSY NMR spectrum of PMP22 in TDPC micelles, pH 5.0 and 45 °C. 128 increments (968 scans each) were recorded, and ^{13}C-decoupling was used. The sweep width was 13.95 ppm in the ^{1}H dimension and 38.52 ppm in the ^{15}N dimension. The peaks numbered 1−10 in the upper part of the spectrum appear to represent 10 of PMP22's 11 glycine residues (numbering does not, of course, correspond to residue number). It should be noted that the extra satellite peaks appearing around peaks 1 and 7 are actually artifacts resulting from the Gaussian apodization function used in the processing of the NMR data. Interactive examination of this spectrum when processed using more than one apodization function leads to confidence in this Gly peak count. From the same examination, it is not clear that either of the two very small peaks between 7 and 10 is a real peak. (B) Close-up view of the tryptophan indole N−H region from the same spectrum as 5A.

detergent solutions tested with the exception of LDAO, in which the protein aggregated before an NMR spectrum could be acquired.

NMR spectra were acquired at two pH values, 6.5 and 5.0, at 45 °C for each detergent. In DPC, lower temperatures were tested (25 and 37 °C), but led to significant reductions in the number of peaks (data not shown). In general, more peaks were observed at pH 5.0 than at pH 6.5, a fact that may reflect a tendency for PMP22 to form higher oligomers or aggregates at neutral pH and/or a lower degree of stable tertiary structure at the higher pH value (as suggested by near-UV CD). We also varied the concentration of PMP22 in the NMR samples after noticing that highly concentrated samples tended to be extremely viscous. Reducing the pH of the samples tends to lower the viscosity, but even at pH 5.0 samples >1.5 mM were very viscous. Optimum conditions for NMR were judged to be 1.0 mM PMP22 in TDPC micelles, at pH 5.0 and 45 °C (see Figure 5). Under these conditions, ca. 150 backbone amide peaks were observed, fully 89% of the ideal 168 (total number of residues minus the number of Pro). PMP22's TROSY resonances display modest chemical shift dispersion in the proton dimension and varying line widths. In these regards, the spectrum is similar to those reported from other folded multispan alpha-helical membrane proteins (*75*−*83*). PMP22 contains 11 glycines. It is therefore reassuring that there are 10 clearly observable peaks in the Gly region of the spectrum (see peaks numbered 1−10, Figure 5A). Moreover, there are six tryptophan residues in the recombinant protein: three in loop regions, two in interfacial regions, and one in a transmembrane helix (see Figure 1B). All six tryptophan indole ^{1}H−^{15}N peaks are observed in the TROSY spectrum (Figure 5B).

The NMR results are consistent with the circular dichroism data, which indicates that PMP22 is a folded α-helical membrane protein. The quality of the TROSY spectrum is comparable to (*75, 79, 82*) or even better than (*78*) spectra of other multispan helical membrane proteins of size comparable to PMP22 for which backbone NMR resonance assignments have been completed. This, along with preliminary 3-D HNCA NMR data (Figure 6), supports the feasibility of conducting NMR-based structural studies of PMP22.

DISCUSSION

High Level Expression and Purification of PMP22. As of mid-2007, there are only 11 experimentally determined structures of mammalian integral membrane proteins (*84*). This dearth of structural information reflects, in part, extreme difficulty in obtaining milligram quantities of vertebrate membrane proteins. Indeed, only 2 of those 11 proteins were purified from a recombinant source—the others represent proteins that are highly abundant in their native tissue. Here, it has been demonstrated that human peripheral myelin protein 22 can be expressed at high levels in *E. coli* using a cleavable N-terminal fusion partner protein (*63*). The expres-

sion and purification method employed may be applicable to other membrane proteins, particularly tetraspan membrane proteins, including the TARPs, claudins, and connexins, which share both sequence homology and the same predicted membrane topology as PMP22.

When compared with protocols for obtaining PMP22 from PNS tissue, our method for producing recombinant protein has several advantages. First, *E. coli* expression makes it possible to conveniently obtain *human* PMP22 and also to produce disease-linked mutant forms. Bacterial expression avoids the potential complications of inhomogeneous post-translational modification. Finally, isotopic labeling of PMP22 for NMR is both straightforward and affordable using *E. coli*.

A potential disadvantage of *E. coli* expression is that PMP22 is not subjected to native N-linked glycosylation. This mode of post-translational modification is generally thought to serve as a quality control "stamp" that signals to protein folding quality control the state of foldedness of a nascent protein, leading to ER retention when the protein is deemed "not yet folded" (*85*−*88*). In the case of PMP22, a non-glycosylated mutant exhibited a half-life in model mammalian cell lines similar to that of WT and also trafficked normally, suggesting that the carbohydrate moiety is not required for correct 3-D structure or stability (*64*, *89*). Moreover, the interaction between PMP22 and MPZ did not appear to require the carbohydrate moiety on either protein to be present. We observed that recombinant PMP22 forms dimers in several types of detergent micelles, suggesting that N-glycosylation is not required for the critical dimerization step that is known to occur for native PMP22 early in the secretory pathway (*4*, *64*, *65*). Nevertheless, PMP22's lone *N*-glycan may be important for forming higher oligomers, the functional significance of which has yet to be determined (*64*). Taken together, the available data indicates that the carbohydrate is not particularly important in maintaining the structure of PMP22, for folding, for stability, for dimerization, or for interaction with MPZ, although it may contribute to higher quaternary structure. It is therefore unlikely that the lack of PMP22's native glycan will hinder biophysical characterization of this protein or attempts to correlate the results from such studies with the biology of this disease-linked protein.

Recombinant PMP22 Folds To Form a Mostly-Helical Dimer with Ordered Tertiary Structure. The method used to purify PMP22 involved the initial extraction/dissolution of the recombinant protein using a harsh detergent, Empigen, that is an excellent solubilizing agent, followed by on-column replacement of this surfactant with mild zwitterionic or non-ionic detergents. Following purification, PMP22 was judged by both circular dichroism and NMR to adopt a folded and largely α-helical structure. All 4 putative transmembrane segments of the protein are most likely helical. The conclusion extends previous work in which a 17 amino acid fragment of the first transmembrane segment of PMP22 was subjected to partial structural characterization in organic solvent mixtures (to mimic the bilayer interior) and determined to be helical (*90*).

PMP22 was observed to exhibit a strong tendency to dimerize, even under reducing (DTT-containing) conditions, and goes on to form disulfide-linked dimers under oxidizing conditions. Given that both the lumen of the endoplasmic reticulum (where native PMP22 is known to fold and dimerize) and the extracellular space (where PMP22's extramembrane Cys residues reside) are oxidizing environments, it is feasible that intra- or intermonomer disulfide bonds are present in the native protein, although this has not been observed in PMP22 extracted from myelinated nerves (L. Notterpek, personal communication). That PMP22 exhibits a high propensity for dimerization is believed to be intimately related to the genetically dominant inheritance pattern for Charcot−Marie−Tooth and related neuropathies that are linked to heterozygous mutations in the PMP22 gene (*64*, *65*). It is believed that mutations in one allele for PMP22 result in misassembly of the mutant protein, but that the misfolded mutant can still form avid heterodimers with the wild type allele-encoded PMP22, leading to ER quality-control-based targeting of *both* WT/mutant gene products for extrusion from the ER (*64*, *65*), leading either to degradation or accumulation as toxic intracellular aggregates (review in ref *4*). It is remarkable that a membrane protein that is judged to be folding-defective by ER quality control is still competent to form dimers with the wild type protein. The work of this paper will enable future studies of the structural and energetic basis for heterodimerization between wild type and disease mutant forms of PMP22.

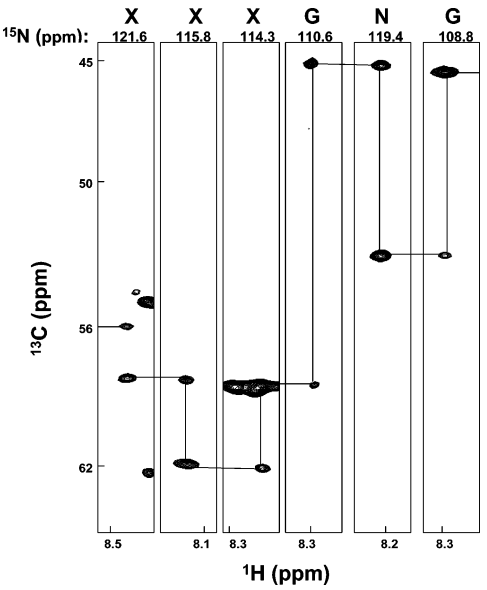

FIGURE 6: Slices from different ^{15}N planes of a constant time HNCA spectrum of PMP22. Sample conditions were the same as for Figure 5. 128 and 192 increments were collected for the ^{15}N and ^{13}C dimensions, respectively. Because PMP22 contains only a single GXG motif and because the glycine peaks are easily identifiable based on their distinctive chemical shifts, it is possible to tentatively assign these resonances as arising from sites 31−33 (GNG) and either the three residues immediately prior to, or following this motif in the extracellular domain.

Our analysis of the pH-dependency of the near-UV CD spectrum of PMP22 (see Results) suggests that the variations in the spectra of Figure 4C as a function of pH are most likely due to conformational changes in the extracellular domain, with little change in the structure of the transmembrane domain. This is not surprising. There is only a single residue in the transmembrane domain (His12) that is conceivably titratable over the pH 1−7 range examined in this study. On the other hand, in the extracellular domain there are 9 His/Glu/Asp residues, each of which could

potentially undergo protonation at some point as the pH is reduced from 7 to 1. The fact that the near-UV CD spectrum of PMP22 was seen to be more intense at pH 3 than at more neutral pH values is surprising, since it suggests a higher degree of 3-D structural order at acidic pH values than at more neutral pH values. One possible interpretation is that the 3-D structure is actually well-ordered at both neutral and acidic pH values, but that there are minor pH-dependent structural changes that impact the packing of the Trp residues in a way that results in more intense circular dichroism in the 290−300 nm near-UV range. Another possible explanation is that the structure is indeed more ordered at pH 3 in detergent micelles, and that under micellar conditions this bulk pH value leads to hydronium ion chemical activity at the water−micelle interface that best reflects the chemical activity of hydronium ions near the surfaces of the unusual closely spaced multilamellar environment of compact myelin.

The identification of conditions for maintaining micellar PMP22 in a well-folded form will allow detailed studies of its folding and stability. It is believed that mutation-induced defects in the folding of PMP22 underlie PMP22-linked neuropathy. Charcot−Marie−Tooth is a well-documented example of a human disease caused by protein misassembly that is triggered by changes in sequence or gene dosage. Misassembly of membrane proteins often arises because of point mutations that hinder the proper folding of the protein, such that the mutant protein ultimately reaches its destination in a nonfunctional form, accumulates in the cell as aggregates, or is degraded via the ERAD pathway (*91*). In each instance, the amount of functional protein that reaches the membrane is reduced. Additional negative consequences arise if the misassembled protein is not properly degraded and forms toxic aggregates and/or if the wild type protein is also engaged by the defective mutant to form a complex, as appears to be the case for PMP22. Membrane protein folding mechanisms are beginning to be analyzed in detail, as exemplified by *in vitro* studies on model membrane proteins such as glycophorin A, bacteriorhodopsin, diacylglycerol kinase, DsbB, OmpA, and others (*92*−*97*). The results of this work set the stage for studies to unravel the precise effects of disease-linked point mutants on the stability, folding, and misfolding of PMP22.

Finally, this work provides the basis for focused efforts to characterize the structure of PMP22 using solution NMR or X-ray crystallography. Both CD and NMR spectroscopy indicate that PMP22 adopts a homogeneous folded structural state. Further improvements in NMR spectral quality can be expected following access to 900 MHz field spectrometers and further sample optimization. Even as a 35 kDa dimer that is part of a much larger micellar complex, PMP22 would appear to be within the range of solution NMR's current capabilities as a method to determine protein backbone conformation. Water soluble proteins as large as 82 kDa monomers have now been structurally determined using NMR methods (*98*), and the structures of more than one >30 kDa integral membrane protein are well underway (*75*, *76*, *78*, *79*, *83*, *99*), not to mention several completed structures for 15−30 kDa membrane proteins (*77*, *100*). Particularly exciting is the possibility of using NMR, even qualitatively, to compare the structure and dynamics of wild type PMP22 to peripheral neuropathy-linked mutant forms.

ACKNOWLEDGMENT

We thank members of the Vanderbilt Mass Spectrometry Research Center (David Friedman, Amy Ham, Wade Calcutt, and Dawn Overstreet) for carrying out protein/peptide mass spectrometry, Markus Voehler, Dr. Congbao Kang, and Prof. Frank Sönnichsen for help with NMR, and Susan Meyn for technical assistance. We thank Dr. Laura Mizoue for generating and providing the TEV protease expression system. We are also grateful to Drs. Philipp Berger and Ueli Suter for providing the cDNA for PMP22, to Dr. Jan Sedzik for providing useful comments regarding a draft version of this manuscript, to one of the reviewers for helpful suggestions about the analysis of the near-UV CD data, and to Dr. Richard Breyer for providing the critical pAH1.96 expression vector and also for much lively discussion.

REFERENCES

1. Naef, R., and Suter, U. (1998) Many facets of the peripheral myelin protein PMP22 in myelination and disease, *Microsc. Res. Tech. 41*, 359−371.
2. Snipes, G. J., Suter, U., Welcher, A. A., and Shooter, E. M. (1992) Characterization of a novel peripheral nervous system myelin protein (PMP-22/SR13), *J. Cell Biol. 117*, 225−238.
3. D'Urso, D., and Muller, H. W. (1997) Ins and outs of peripheral myelin protein-22: mapping transmembrane topology and intracellular sorting, *J. Neurosci. Res. 49*, 551−562.
4. Sanders, C. R., Ismail-Beigi, F., and McEnery, M. W. (2001) Mutations of peripheral myelin protein 22 result in defective trafficking through mechanisms which may be common to diseases involving tetraspan membrane proteins, *Biochemistry 40*, 9453−9459.
5. Van Itallie, C. M., and Anderson, J. M. (2006) Claudins and epithelial paracellular transport, *Annu. Rev. Physiol. 68*, 403−429.
6. Taylor, V., Zgraggen, C., Naef, R., and Suter, U. (2000) Membrane topology of peripheral myelin protein 22, *J. Neurosci. Res. 62*, 15−27.
7. Jetten, A. M., and Suter, U. (2000) The peripheral myelin protein 22 and epithelial membrane protein family, *Prog. Nucleic Acid Res. Mol. Biol. 64*, 97−129.
8. Ohsawa, Y., Murakami, T., Miyazaki, Y., Shirabe, T., and Sunada, Y. (2006) Peripheral myelin protein 22 is expressed in human central nervous system, *J. Neurol. Sci. 247*, 11−15.
9. Suter, U., Snipes, G. J., Schoener-Scott, R., Welcher, A. A., Pareek, S., Lupski, J. R., Murphy, R. A., Shooter, E. M., and Patel, P. I. (1994) Regulation of tissue-specific expression of alternative peripheral myelin protein-22 (PMP22) gene transcripts by two promoters, *J. Biol. Chem. 269*, 25795−25808.
10. Adlkofer, K., Martini, R., Aguzzi, A., Zielasek, J., Toyka, K. V., and Suter, U. (1995) Hypermyelination and demyelinating peripheral neuropathy in Pmp22-deficient mice, *Nat. Genet. 11*, 274−280.
11. Bronstein, J. M. (2000) Function of tetraspan proteins in the myelin sheath, *Curr. Opin. Neurobiol. 10*, 552−557.
12. Carenini, S., Neuberg, D., Schachner, M., Suter, U., and Martini, R. (1999) Localization and functional roles of PMP22 in peripheral nerves of P0-deficient mice, *Glia 28*, 256−264.
13. Quarles, R. H. (2002) Myelin sheaths: glycoproteins involved in their formation, maintenance and degeneration, *Cell. Mol. Life Sci. 59*, 1851−1871.
14. Amici, S. A., Dunn, W. A., Jr., and Notterpek, L. (2007) Developmental abnormalities in the nerves of peripheral myelin protein 22-deficient mice, *J. Neurosci. Res. 85*, 238−249.
15. Arroyo, E. J., and Scherer, S. S. (2000) On the molecular architecture of myelinated fibers, *Histochem. Cell Biol. 113*, 1−18.
16. Scherer, S. S., and Arroyo, E. J. (2002) Recent progress on the molecular organization of myelinated axons, *J. Peripher. Nerv. Syst. 7*, 1−12.
17. Shy, M. E. (2006) Peripheral neuropathies caused by mutations in the myelin protein zero, *J. Neurol. Sci. 242*, 55−66.
18. D'Urso, D., Ehrhardt, P., and Muller, H. W. (1999) Peripheral myelin protein 22 and protein zero: a novel association in peripheral nervous system myelin, *J. Neurosci. 19*, 3396−3403.

19. Hasse, B., Bosse, F., Hanenberg, H., and Muller, H. W. (2004) Peripheral myelin protein 22 kDa and protein zero: domain specific trans-interactions, *Mol. Cell Neurosci. 27*, 370−378.
20. Shapiro, L., Doyle, J. P., Hensley, P., Colman, D. R., and Hendrickson, W. A. (1996) Crystal structure of the extracellular domain from P-0, the major structural protein of peripheral nerve myelin, *Neuron 17*, 435−449.
21. Zoidl, G., Blass-Kampmann, S., D'Urso, D., Schmalenbach, C., and Muller, H. W. (1995) Retroviral-mediated gene transfer of the peripheral myelin protein PMP22 in Schwann cells: modulation of cell growth, *EMBO J. 14*, 1122−1128.
22. Roux, K. J., Amici, S. A., Fletcher, B. S., and Notterpek, L. (2005) Modulation of epithelial morphology, monolayer permeability, and cell migration by growth arrest specific 3/peripheral myelin protein 22, *Mol. Biol. Cell 16*, 1142−1151.
23. Atanasoski, S., Scherer, S. S., Nave, K. A., and Suter, U. (2002) Proliferation of Schwann cells and regulation of cyclin D1 expression in an animal model of Charcot-Marie-Tooth disease type 1A, *J. Neurosci. Res. 67*, 443−449.
24. Giambonini-Brugnoli, G., Buchstaller, J., Sommer, L., Suter, U., and Mantei, N. (2005) Distinct disease mechanisms in peripheral neuropathies due to altered peripheral myelin protein 22 gene dosage or a Pmp22 point mutation, *Neurobiol. Dis. 18*, 656−668.
25. Notterpek, L., Snipes, G. J., and Shooter, E. M. (1999) Temporal expression pattern of peripheral myelin protein 22 during in vivo and in vitro myelination, *Glia 25*, 358−369.
26. Notterpek, L., Roux, K. J., Amici, S. A., Yazdanpour, A., Rahner, C., and Fletcher, B. S. (2001) Peripheral myelin protein 22 is a constituent of intercellular junctions in epithelia, *Proc. Natl. Acad. Sci. U.S.A. 98*, 14404−14409.
27. Amici, S. A., Dunn, W. A., Jr., Murphy, A. J., Adams, N. C., Gale, N. W., Valenzuela, D. M., Yancopoulos, G. D., and Notterpek, L. (2006) Peripheral myelin protein 22 is in complex with alpha6beta4 integrin, and its absence alters the Schwann cell basal lamina, *J. Neurosci. 26*, 1179−1189.
28. Nicoll, R. A., Tomita, S., and Bredt, D. S. (2006) Auxiliary subunits assist AMPA-type glutamate receptors, *Science 311*, 1253−1256.
29. Ziff, E. B. (2007) TARPs and the AMPA receptor trafficking paradox, *Neuron 53*, 627−633.
30. Hua, V. B., Chang, A. B., Tchieu, J. H., Kumar, N. M., Nielsen, P. A., and Saier, M. H., Jr. (2003) Sequence and phylogenetic analyses of 4 TMS junctional proteins of animals: connexins, innexins, claudins and occludins, *J. Membr. Biol. 194*, 59−76.
31. Takeda, Y., Notsu, T., Kitamura, K., and Uyemura, K. (2001) Functional analysis for peripheral myelin protein PASII/PMP22: is it a member of claudin superfamily?, *Neurochem. Res. 26*, 599−607.
32. Evans, W. H., De, V. E., and Leybaert, L. (2006) The gap junction cellular internet: connexin hemichannels enter the signalling limelight, *Biochem. J. 397*, 1−14.
33. Koval, M. (2006) Pathways and control of connexin oligomerization, *Trends Cell Biol. 16*, 159−166.
34. Sosinsky, G. E., and Nicholson, B. J. (2005) Structural organization of gap junction channels, *Biochim. Biophys. Acta 1711*, 99−125.
35. Berger, P., Niemann, A., and Suter, U. (2006) Schwann cells and the pathogenesis of inherited motor and sensory neuropathies (Charcot-Marie-Tooth disease), *Glia 54*, 243−257.
36. Suter, U., and Scherer, S. S. (2003) Disease mechanisms in inherited neuropathies, *Nat. Rev. Neurosci. 4*, 714−726.
37. Saifi, G. M., Szigeti, K., Snipes, G. J., Garcia, C. A., and Lupski, J. R. (2003) Molecular mechanisms, diagnosis, and rational approaches to management of and therapy for Charcot-Marie-Tooth disease and related peripheral neuropathies, *J. Invest. Med. 51*, 261−283.
38. Colby, J., Nicholson, R., Dickson, K. M., Orfali, W., Naef, R., Suter, U., and Snipes, G. J. (2000) PMP22 carrying the trembler or trembler-J mutation is intracellularly retained in myelinating Schwann cells, *Neurobiol. Dis. 7*, 561−573.
39. D'Urso, D., Prior, R., Greiner-Petter, R., Gabreels-Festen, A. A., and Muller, H. W. (1998) Overloaded endoplasmic reticulum-Golgi compartments, a possible pathomechanism of peripheral neuropathies caused by mutations of the peripheral myelin protein PMP22, *J. Neurosci. 18*, 731−740.
40. Fortun, J., Dunn, W. A., Jr., Joy, S., Li, J., and Notterpek, L. (2003) Emerging role for autophagy in the removal of aggresomes in Schwann cells, *J. Neurosci. 23*, 10672−10680.
41. Fortun, J., Li, J., Go, J., Fenstermaker, A., Fletcher, B. S., and Notterpek, L. (2005) Impaired proteasome activity and accumulation of ubiquitinated substrates in a hereditary neuropathy model, *J. Neurochem. 92*, 1531−1541.
42. Naef, R., and Suter, U. (1999) Impaired intracellular trafficking is a common disease mechanism of PMP22 point mutations in peripheral neuropathies, *Neurobiol. Dis. 6*, 1−14.
43. Notterpek, L., Ryan, M. C., Tobler, A. R., and Shooter, E. M. (1999) PMP22 accumulation in aggresomes: implications for CMT1A pathology, *Neurobiol. Dis. 6*, 450−460.
44. Ryan, M. C., Shooter, E. M., and Notterpek, L. (2002) Aggresome formation in neuropathy models based on peripheral myelin protein 22 mutations, *Neurobiol. Dis. 10*, 109−118.
45. Tobler, A. R., Liu, N., Mueller, L., and Shooter, E. M. (2002) Differential aggregation of the Trembler and Trembler J mutants of peripheral myelin protein 22, *Proc. Natl. Acad. Sci. U.S.A. 99*, 483−488.
46. Liu, N., Yamauchi, J., and Shooter, E. M. (2004) Recessive, but not dominant, mutations in peripheral myelin protein 22 gene show unique patterns of aggregation and intracellular trafficking, *Neurobiol. Dis. 17*, 300−309.
47. Robaglia-Schlupp, A., Pizant, J., Norreel, J. C., Passage, E., Saberan-Djoneidi, D., Ansaldi, J. L., Vinay, L., Figarella-Branger, D., Levy, N., Clarac, F., Cau, P., Pellissier, J. F., and Fontes, M. (2002) PMP22 overexpression causes dysmyelination in mice, *Brain 125*, 2213−2221.
48. Huxley, C., Passage, E., Robertson, A. M., Youl, B., Huston, S., Manson, A., Saberan-Djoniedi, D., Figarella-Branger, D., Pellissier, J. F., Thomas, P. K., and Fontes, M. (1998) Correlation between varying levels of PMP22 expression and the degree of demyelination and reduction in nerve conduction velocity in transgenic mice, *Hum. Mol. Genet. 7*, 449−458.
49. Sereda, M. W., and Nave, K. A. (2006) Animal models of Charcot-Marie-Tooth disease type 1A, *Neuromol. Med. 8*, 205−216.
50. Fortun, J., Go, J. C., Li, J., Amici, S. A., Dunn, W. A., Jr., and Notterpek, L. (2006) Alterations in degradative pathways and protein aggregation in a neuropathy model based on PMP22 overexpression, *Neurobiol. Dis. 22*, 153−164.
51. Pareek, S., Notterpek, L., Snipes, G. J., Naef, R., Sossin, W., Laliberte, J., Iacampo, S., Suter, U., Shooter, E. M., and Murphy, R. A. (1997) Neurons promote the translocation of peripheral myelin protein 22 into myelin, *J. Neurosci. 17*, 7754−7762.
52. Kitamura, K., Suzuki, M., and Uyemura, K. (1976) Purification and partial characterization of two glycoproteins in bovine peripheral nerve myelin membrane, *Biochim. Biophys. Acta 455*, 806−816.
53. Sedzik, J., Kotake, Y., and Uyemura, K. (1998) Purification of PASII/PMP22−an extremely hydrophobic glycoprotein of PNS myelin membrane, *Neuroreport 9*, 1595−1600.
54. Sedzik, J., Uyemura, K., and Tsukihara, T. (2002) Towards crystallization of hydrophobic myelin glycoproteins: P0 and PASII/PMP22, *Protein Expression Purif. 26*, 368−377.
55. Kapust, R. B., Tozser, J., Fox, J. D., Anderson, D. E., Cherry, S., Copeland, T. D., and Waugh, D. S. (2001) Tobacco etch virus protease: mechanism of autolysis and rational design of stable mutants with wild-type catalytic proficiency, *Protein Eng. 14*, 993−1000.
56. Schmidt, T. G., and Skerra, A. (1994) One-step affinity purification of bacterially produced proteins by means of the "Strep tag" and immobilized recombinant core streptavidin, *J. Chromatogr. A 676*, 337−345.
57. Anumanthan, G., Halder, S. K., Friedman, D. B., and Datta, P. K. (2006) Oncogenic serine-threonine kinase receptor-associated protein modulates the function of Ewing sarcoma protein through a novel mechanism, *Cancer Res. 66*, 10824−10832.
58. Bender, R. P., Ham, A. J., and Osheroff, N. (2007) Quinone-induced enhancement of DNA cleavage by human topoisomerase IIalpha: adduction of cysteine residues 392 and 405, *Biochemistry 46*, 2856−2864.
59. Weigelt, J., Miles, C. S., Dixon, N. E., and Otting, G. (1998) Backbone NMR assignments and secondary structure of the N-terminal domain of DnaB helicase from E. coli, *J. Biomol. NMR 11*, 233−234.
60. Salzmann, M., Pervushin, K., Wider, G., Senn, H., and Wuthrich, K. (1999) [13C]-constant-time [15N,1H]-TROSY-HNCA for sequential assignments of large proteins, *J. Biomol. NMR 14*, 85−88.
61. Delaglio, F., Grzesiek, S., Vuister, G. W., Zhu, G., Pfeifer, J., and Bax, A. (1995) NMRPipe: a multidimensional spectral processing system based on UNIX pipes, *J. Biomol. NMR 6*, 277−293.

62. Ritz, M. F., Lechner-Scott, J., Scott, R. J., Fuhr, P., Malik, N., Erne, B., Taylor, V., Suter, U., Schaeren-Wiemers, N., and Steck, A. J. (2000) Characterisation of autoantibodies to peripheral myelin protein 22 in patients with hereditary and acquired neuropathies, *J. Neuroimmunol. 104*, 155−163.
63. Breyer, R. M., Ma, L., and Kennedy, C. (2002) Methods and compositions for high yield production of eukaryotic proteins, U.S. Patent 6,383,777.
64. Ryan, M. C., Notterpek, L., Tobler, A. R., Liu, N., and Shooter, E. M. (2000) Role of the peripheral myelin protein 22 N-linked glycan in oligomer stability, *J. Neurochem. 75*, 1465−1474.
65. Tobler, A. R., Notterpek, L., Naef, R., Taylor, V., Suter, U., and Shooter, E. M. (1999) Transport of Trembler-J mutant peripheral myelin protein 22 is blocked in the intermediate compartment and affects the transport of the wild-type protein by direct interaction, *J. Neurosci. 19*, 2027−2036.
66. Tobler, A. R., Liu, N., Mueller, L., and Shooter, E. M. (2002) Differential aggregation of the Trembler and Trembler J mutants of peripheral myelin protein 22, *Proc. Natl. Acad. Sci. U.S.A. 99*, 483−488.
67. Andrade, M. A., Chacon, P., Merelo, J. J., and Moran, F. (1993) Evaluation of secondary structure of proteins from UV circular dichroism spectra using an unsupervised learning neural network, *Protein Eng. 6*, 383−390.
68. Wu, C. S., Ikeda, K., and Yang, J. T. (1981) Ordered conformation of polypeptides and proteins in acidic dodecyl sulfate solution, *Biochemistry 20*, 566−570.
69. Batenjany, M. M., Mizukami, H., and Salhany, J. M. (1993) Near-UV circular dichroism of band 3. Evidence for intradomain conformational changes and interdomain interactions, *Biochemistry 32*, 663−668.
70. Brouillette, C. G., McMichens, R. B., Stern, L. J., and Khorana, H. G. (1989) Structure and thermal stability of monomeric bacteriorhodopsin in mixed phospholipid/detergent micelles, *Proteins 5*, 38−46.
71. Taylor, R. M., Zakharov, S. D., Bernard, H. J., Girvin, M. E., and Cramer, W. A. (2000) Folded state of the integral membrane colicin E1 immunity protein in solvents of mixed polarity, *Biochemistry 39*, 12131−12139.
72. Turk, E., Gasymov, O. K., Lanza, S., Horwitz, J., and Wright, E. M. (2006) A reinvestigation of the secondary structure of functionally active vSGLT, the vibrio sodium/galactose cotransporter, *Biochemistry 45*, 1470−1479.
73. Woody, R. W., and Dunker, A. K. (1996) Aromatic and cystine side-chain circular dichroism in proteins, in *Circular dichroism and the conformational analysis of biomolecules* (Fasman, G. D., Ed.) pp 109−157, Plenum Press, New York.
74. Kelly, S. M., and Price, N. C. (2000) *The use of circular dichroism in the investigation of protein structure and function*, 1st ed., pp 349−284.
75. Chill, J. H., Louis, J. M., Miller, C., and Bax, A. (2006) NMR study of the tetrameric KcsA potassium channel in detergent micelles, *Protein Sci. 15*, 684−698.
76. Koglin, A., Klammt, C., Trbovic, N., Schwarz, D., Schneider, B., Schafer, B., Lohr, F., Bernhard, F., and Dotsch, V. (2006) Combination of cell-free expression and NMR spectroscopy as a new approach for structural investigation of membrane proteins, *Magn Reson. Chem. 44 Spec No.*, S17−S23.
77. Tamm, L. K., and Liang, B. Y. (2006) NMR of membrane proteins in solution, *Prog. Nucl. Magn. Reson. Spectrosc. 48*, 201−210.
78. Trbovic, N., Klammt, C., Koglin, A., Lohr, F., Bernhard, F., and Dotsch, V. (2005) Efficient strategy for the rapid backbone assignment of membrane proteins, *J. Am. Chem. Soc. 127*, 13504−13505.
79. Oxenoid, K., Kim, H. J., Jacob, J., Sonnichsen, F. D., and Sanders, C. R. (2004) NMR assignments for a helical 40 kDa membrane protein, *J. Am. Chem. Soc. 126*, 5048−5049.
80. Columbus, L., Lipfert, J., Klock, H., Millett, I., Doniach, S., and Lesley, S. A. (2006) Expression, purification, and characterization of Thermotoga maritima membrane proteins for structure determination, *Protein Sci. 15*, 961−975.
81. Page, R. C., Moore, J. D., Nguyen, H. B., Sharma, M., Chase, R., Gao, F. P., Mobley, C. K., Sanders, C. R., Ma, L., Sonnichsen, F. D., Lee, S., Howell, S. C., Opella, S. J., and Cross, T. A. (2006) Comprehensive evaluation of solution nuclear magnetic resonance spectroscopy sample preparation for helical integral membrane proteins, *J. Struct. Funct. Genomics 7*, 51−64.
82. Poget, S. F., Cahill, S. M., and Girvin, M. E. (2007) Isotropic bicelles stabilize the functional form of a small multidrug-resistance pump for NMR structural studies, *J. Am. Chem. Soc. 129*, 2432−2433.
83. Takeuchi, K., Takahashi, H., Kawano, S., and Shimada, I. (2007) Identification and characterization of the slowly exchanging pH-dependent conformational rearrangement in KcsA, *J. Biol. Chem. 282*, 15179−15186.
84. White, S. H. (2005) Membrane proteins of known 3-D structure.
85. Ruddock, L. W., and Molinari, M. (2006) N-glycan processing in ER quality control, *J. Cell Sci. 119*, 4373−4380.
86. Ellgaard, L., and Helenius, A. (2003) Quality control in the endoplasmic reticulum, *Nat. Rev. Mol. Cell Biol. 4*, 181−191.
87. Helenius, A., and Aebi, M. (2004) Roles of N-linked glycans in the endoplasmic reticulum, *Annu. Rev. Biochem. 73*, 1019−1049.
88. Dickson, K. M., Bergeron, J. J., Shames, I., Colby, J., Nguyen, D. T., Chevet, E., Thomas, D. Y., and Snipes, G. J. (2002) Association of calnexin with mutant peripheral myelin protein-22 ex vivo: a basis for "gain-of-function" ER diseases, *Proc. Natl. Acad. Sci. U.S.A. 99*, 9852−9857.
89. Fontanini, A., Chies, R., Snapp, E. L., Ferrarini, M., Fabrizi, G. M., and Brancolini, C. (2005) Glycan-independent role of calnexin in the intracellular retention of Charcot-Marie-tooth 1A Gas3/PMP22 mutants, *J. Biol. Chem. 280*, 2378−2387.
90. Yamada, K., Sato, J., Oku, H., and Katakai, R. (2003) Conformation of the transmembrane domains in peripheral myelin protein 22. Part 1. Solution-phase synthesis and circular dichroism study of protected 17-residue partial peptides in the first putative transmembrane domain, *J. Pept. Res. 62*, 78−87.
91. Sanders, C. R., and Myers, J. K. (2004) Disease-related misassembly of membrane proteins, *Annu. Rev. Biophys. Biomol. Struct. 33*, 25−51.
92. Lorch, M., and Booth, P. J. (2004) Insertion kinetics of a denatured alpha helical membrane protein into phospholipid bilayer vesicles, *J. Mol. Biol. 344*, 1109−1121.
93. Mi, D., Kim, H. J., Hadziselimovic, A., and Sanders, C. R. (2006) Irreversible misfolding of diacylglycerol kinase is independent of aggregation and occurs prior to trimerization and membrane association, *Biochemistry 45*, 10072−10084.
94. Nagy, J. K., Lonzer, W. L., and Sanders, C. R. (2001) Kinetic study of folding and misfolding of diacylglycerol kinase in model membranes, *Biochemistry 40*, 8971−8980.
95. Nagy, J. K., and Sanders, C. R. (2004) Destabilizing mutations promote membrane protein misfolding, *Biochemistry 43*, 19−25.
96. Otzen, D. E. (2003) Folding of DsbB in mixed micelles: a kinetic analysis of the stability of a bacterial membrane protein, *J. Mol. Biol. 330*, 641−649.
97. Sehgal, P., and Otzen, D. E. (2006) Thermodynamics of unfolding of an integral membrane protein in mixed micelles, *Protein Sci. 15*, 890−899.
98. Tugarinov, V., Choy, W. Y., Orekhov, V. Y., and Kay, L. E. (2005) Solution NMR-derived global fold of a monomeric 82-kDa enzyme, *Proc. Natl. Acad. Sci. U.S.A. 102*, 622−627.
99. Malia, T. J., and Wagner, G. (2007) NMR structural investigation of the mitochondrial outer membrane protein VDAC and its interaction with antiapoptotic Bcl-xL, *Biochemistry 46*, 514−525.
100. Sanders, C. R., and Sonnichsen, F. (2006) Solution NMR of membrane proteins: practice and challenges, *Magn Reson. Chem. 44 Spec No.*, S24−S40.
101. Stenson, P. D., Ball, E. V., Mort, M., Phillips, A. D., Shiel, J. A., Thomas, N. S., Abeysinghe, S., Krawczak, M., and Cooper, D. N. (2003) Human Gene Mutation Database (HGMD(R)): 2003 update, *Hum. Mutat. 21*, 577−581.

BI700855J